Heliyon 10 (2024) e39412

Contents lists available at ScienceDirect

Heliyon

journal homepage: www.cell.com/heliyon

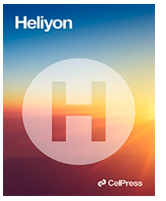

Research article

Physico-mechanical characterization and DFT studies of benzoyl peroxide treated water hyacinth reinforced polypropylene composites

Kaniz Fatema [a], Taslima Akter [a], Zahidul Islam [b], Mohammad Shahriar Bashar [c], Shahin Sultana [b,*], M. Saiful Islam [a,**]

[a] Department of Theoretical and Computational Chemistry, University of Dhaka, Dhaka, 1000, Bangladesh
[b] Fiber and Polymer Research Division, BCSIR Dhaka Laboratories, Bangladesh Council of Scientific and Industrial Research (BCSIR), Dhaka, 1205, Bangladesh
[c] Institute of Energy Research and Development, Bangladesh Council of Scientific and Industrial Research (BCSIR), Dhaka, 1205, Bangladesh

ARTICLE INFO

Keywords:
Polypropylene
Water hyacinth
Composites
Tensile strength
DFT

ABSTRACT

The use of eco-friendly natural fiber-reinforced polymer composites is rapidly expanding across diverse sectors. The rapid spread of water hyacinth disrupts aquatic ecosystems by modifying the pH of water and salinity in Bangladesh. This work investigated on the impact of incorporating both untreated and chemically treated water hyacinth fibers into polypropylene (PP). Untreated water hyacinth (UWH) powder was treated with an alkaline solution, producing mercerized water hyacinth (MWH). MWH was further oxidized to yield oxidized water hyacinth (OWH). Analysis of attenuated total reflection-fourier transform infrared (ATR-FTIR) spectra of UWH, MWH and OWH confirmed cellulose modification. The UWH and OWH were taken in varying contents (1, 2.5, 5, 7.5, and 10 wt%) and added to PP to make UWH-PP and OWH-PP composites using compression molding technique. The 1 % fiber content OWH-PP composites exhibited enhanced tensile strength, elongation, and impact strength compared to UWH-PP composites. Enhanced mechanical properties in OWH-PP composites suggested that benzoyl peroxide treatment improves interfacial adhesion. Morphological analysis of the OWH-PP composite showed better interfacial bonding between water hyacinth and PP than that of the UWH-PP composite. Thermogravimetric analysis (TGA) depicted the thermal stability of the UWH-PP and OWH-PP composites. The chemical reaction of cellulose monomer was further studied with DFT/B3LYP level of theory using two different basis sets 6-31+G(d, p) and cc-pVTZ. The calculated vibrational spectra of the untreated, mercerized and oxidized cellulose monomer agree well with the ATR-FTIR spectra, confirming chemical modification. DFT calculations of thermodynamic properties revealed the feasibility of the reactions. Electronic property (NBO charge) indicated charge transfer and structural changes during chemical modification.

* Corresponding author.
** Corresponding author.
E-mail addresses: shasultana@gmail.com (S. Sultana), dr.mdsaifulislam@yahoo.com (M.S. Islam).

https://doi.org/10.1016/j.heliyon.2024.e39412
Received 18 August 2024; Received in revised form 7 October 2024; Accepted 14 October 2024
Available online 15 October 2024

1. Introduction

The imperative need to address environmental concerns and safeguard natural resources has led to a significant shift in exploring and creating natural materials derived from renewable sources. This endeavor is not just an option but a compelling necessity in our pursuit of secure and sustainable living. Industries, recognizing the ecological challenges posed by synthetic material-based composites, are now actively directing their efforts toward the use of plant fiber reinforcements [1]. The exceptional characteristics of natural fibers, including their abundance, cost-effective and easy processing, non-toxicity, versatility, high performance, and non-irritating nature to the respiratory system, skin, and eyes, as well as their non-corrosive properties, make them highly advantageous. Additionally, in comparison to synthetic fibers such as glass fibers, natural fibers require 17 % less energy during production, further enhancing their appeal. Utilizing these composites in numerous areas can increase manufacturing speed and recycling while remaining environmentally friendly [2,3].

Natural fiber-reinforced polymer composites exhibit remarkable qualities, making them promising across industries, especially in automotive and civil infrastructure [4]. These composites enhance dashboards, door panels, seats, and cabin linings in automotive applications because of their exceptional stiffness-to-weight and strength-to-weight ratios. Recognized for commendable mechanical attributes, they significantly contribute to the structural integrity and performance of automotive elements. Comparing natural fibers to synthetic ones, their favourable characteristics, cost-effectiveness, and eco-friendly processing of natural fibers position them as viable alternatives in polymeric composites, showing significant potential in load-bearing applications and packaging [4,5].

Polypropylene (PP) is a versatile thermoplastic commonly employed in packaging, automotive, and construction for its cost-effectiveness and low density. With strong mechanical strength, high impact resistance, and outstanding chemical resistance, PP is soluble in polar media, making it ideal for specific applications. The microcrystalline structure inherent in PP influences its overall properties. Additionally, PP exhibits compatibility with diverse materials, like microcrystalline cellulose, enhancing its properties [6,7].

Water hyacinth, an aquatic weed, is globally recognized as an invasive species due to its rapid growth, forming substantial layers on water surfaces [8]. These plants not only alter the pH and salinity of water but also induce an imbalance, modifying the physical and chemical properties of entire aquatic ecosystems. A few years back, water hyacinth was introduced in Bengal for its aesthetically pleasing flowers and leaves. However, the extensive proliferation of this species resulted in the devastation of fish, other aquatic fauna, and indigenous water plants. Consequently, it earned the moniker "Bengal terror." [9]. Despite facing obstacles, the considerable fiber concentration of water hyacinth (up to 20 % by weight) positions it as a plausible resource for both composite and textile sectors. This presents opportunities for its environmentally conscious application as a raw material, emphasizing sustainability in its utilization [8]. Water hyacinth fiber-reinforced polymer composites possess acceptable mechanical properties for concrete strengthening purposes. Moreover, Water hyacinth fiber-reinforced polymer composites are more environmentally friendly than conventional composites, as their production requires less water and generates less waste [10].

This research used water hyacinth (Eichhornia crassipes) as a reinforcing material with Polypropylene (PP), a widely used thermoplastic polymer as matrix for composite fabrication by compression molding technique. Though originating in North America, Africa, Europe, and new lands, water hyacinth is rapidly proliferating in Bangladesh's wetlands and poses challenges and potential opportunities. So, one of the primary objectives of this research is to investigate the utilization of water hyacinth sourced from Bangladesh as a fundamental component in the manufacturing of composite materials.

The inherent moisture absorption capacity of natural fibers presents a significant challenge in the domain of natural fiber-reinforced composites. This high moisture uptake leads to swelling and reduced dimensional stability upon exposure to water [11]. This, in turn, induces micro-crack development, causing mechanical failure and hindering widespread applications [12]. The uneven dispersion of water molecules within composites further compromises their physical and mechanical properties, exacerbating the issue [13]. The tendency of natural fibers to absorb moisture presents obstacles to the resilience and functionality of composites reinforced with natural fibers. This underscores the essential requirement for efficient treatments and surface modifications to counteract these challenges [14,15]. Addressing these challenges, chemical treatments emerge as effective solutions. They enhance mechanical properties, reduce moisture absorption, and improve interfacial adhesion. The alteration of fiber microstructure achieves superior tensile strength, refined wettability, and modified surface morphology [16]. By reducing the lignin and hemicellulose content while retaining a considerable amount of cellulose, chemical treatments can preserve the essential properties of natural fibers while making them more resistant to water [17].

Masłowski et al. investigated peroxide modifications on cereal straw and natural rubber composites. Using both alkaline and peroxide treatments, they modified cereal straw fibers, employing them as cellulosic fillers in natural rubber biocomposites [18]. Taslima et al. investigated the mechanical properties of benzoyl peroxide-treated teak sawdust-polypropylene (PP) composites. The treated composites demonstrated superior tensile and impact strength compared to their untreated counterparts, along with enhanced water uptake behaviour [5]. V. Kumar et al. conducted experiments on bamboo-glass fiber hybrid composites, varying lamina arrangements and assessing their viability for structural applications through tests on tensile, flexural, and impact strength [19]. Imtiaz et al. developed jute fiber-reinforced polypropylene composites treated with sodium periodate, revealing enhanced thermal resistance and improved compatibility with the matrix [18]. Haque et al. discussed coir fiber treatment with 20 % w/v aqueous sodium periodate solutions, highlighting its use in green polymer composites [20] In 2010, Supri and Ismail pioneered a low-density polyethylene/water hyacinth (LDPE/WH) composite, improving tensile strength, water absorption resistance, and thermal stability [8]. Sumrith et al. characterized water hyacinth fibers treated with NaOH and silane, demonstrating their potential as reinforced materials in bioepoxy-based sustainable composites [21]. Ramirez et al. demonstrated the economical production of composites using water hyacinth and polyester resin, enhancing thermal and mechanical properties [22].

As per our current understanding, there exists a research gap in the chemical modification of cellulose derived from water hyacinth to benzoyloxy cellulose. To date, no scholarly investigations have explored the process of chemically treating cellulose of water hyacinth to yield benzoyloxy cellulose.

Kaushik et al. [23] studied mercerization and benzoyl peroxide treatment effects on sisal fibers, finding enhanced thermal stability and crystallinity. In a similar vein, this study investigates the influences of benzoyl peroxide treatment and the content of water hyacinth on the physico-mechanical properties of water hyacinth powder (WHP) reinforced PP composites, with detailed findings presented in the paper. Water hyacinth comprises cellulose, lignin and hemicellulose, which possess abundant functional groups, particularly hydroxyls. This research focuses on modifying water hyacinth cellulose to benzoyloxy cellulose using benzoyl peroxide. Taking a step further, molecular optimization is performed through Density Functional Theory (DFT) with B3LYP functional, cc-pVTZ, and 6-31G + (d,p) basis sets. DFT analyses cover thermodynamic properties, Natural Bond Orbital (NBO) charges and vibrational spectra, confirming reaction feasibility and providing insights into induced structural and chemical changes induced by the treatment process. This multifaceted approach combines experimental results with theoretical insights, offering a holistic understanding of the water hyacinth-reinforced PP composites and their potential applications in environmentally conscious material science.

2. Experimental

2.1. Materials

A commercial grade polypropylene (PP) was used in the study. It was manufactured by Saudi Polymers Company in Al Jubail, Kingdom of Saudi Arabia. The melting point of polypropylene was determined to be 162 °C. The water hyacinth (*Eichornia crassipes*) was collected from Rajarbagh, Basabo, Dhaka, Bangladesh. The height of the plants was approximately 2–3 ft. For this investigation, the whole water hyacinth plant was used. Sodium hydroxide (NaOH), benzoyl peroxide $(C_6H_5CO)_2O_2$ chemicals from Merck, Germany and acetone (CH_3COCH_3) from Central Drug House (P) Ltd, Delhi, India were used in this work.

2.2. Processing of untreated water hyacinth powder (UWH)

Several physical techniques, including washing, drying, grinding, sieving and meshing were used to process UWH samples. It was initially washed with tap water to remove all undesirable solid particles, then air-dried in bright sunlight for 25 days in the summer time and was cut into small pieces and oven-dried for 45 min at 95 °C and was ground into powder using the grinder and then UWH was sieved to achieve fine powder. The particle size was determined by sieving it with the specific mesh (mesh 35).

2.3. Surface modification of UWH by chemical treatment

Water hyacinth powder was immersed in a 5 % sodium hydroxide solution at room temperature (25 °C), for an hour. Ratio for UWH to the liquor was 1:20 (w/v). The color of UWH shifted from greenish brown to brown at the end of this alkali treatment yielding mercerized water hyacinth (MWH). The MWH was thoroughly rinsed with distilled water until the pH of the sample was neutral. It was then air-dried for 24 h, followed by drying in a vacuum dryer oven at 60 °C for 12 h to achieve constant weights. The dried MWH was subsequently employed in a modification reaction with 6 % benzoyl peroxide in acetone solution. To obtain a favourable outcome from ATR-FTIR spectroscopic analyses, a few reactions with different duration (30 min, 1 h, 3 h, and 6 h) were conducted for this chemical treatment. The tensile strength of composites indicated a progressive increase with rising concentrations of benzoyl peroxide in the treatment, reaching a peak at 6 %. Following that, the tensile strength reached a point of stability, with no notable further changes. The experiment involved employing a 6 % benzoyl peroxide solution in acetone, and the reaction duration spanned 6 h under standard room temperature (25 °C) conditions and with pH 5.0 after the reaction parameters were chosen. The sample was washed with distilled water until the pH of the sample was neutralized and allowed to dry in the air. Before being combined with the matrix, the OWH was dried in a vacuum dryer oven at 60 °C repeatedly until a constant weight was achieved.

Table 1
Relative amounts of reinforcing materials and polymer matrix in composites.

	Water hyacinth fraction (Reinforcing material) weight %	Polypropylene fraction (Polymer matrix) weight %	Composite polymer weight %
UWH	0.0	100.0	0.0:100.0 PP
	1.0	99.0	1.0:99.0 UWH-PP
	2.5	97.5	2.5:97.5 UWH-PP
	5.0	95.0	5.0:95.0 UWH-PP
	7.5	92.5	7.5:92.5 UWH-PP
	10.0	90.0	10.0:90.0 UWH-PP
OWH	1.0	99.0	1.0:99.0 OWH-PP
	2.5	97.5	2.5:97.5 OWH-PP
	5.0	95.0	5.0:95.0 OWH-PP
	7.5	92.5	7.5:92.5 OWH-PP
	10.0	900	10.0:90.0 OWH-PP

2.4. Attenuated total reflection-fourier transform infrared (ATR-FTIR) spectroscopic characterization of UWH, MWH and OWH

On a Fourier transform spectrophotometer, *Frontier*™ by PerkinElmer, the ATR-FTIR spectra of UWH, MWH and OWH were recorded at the range of frequency range 4000–650 cm^{-1}. Approximately 0.5 mg of powdered samples were taken to obtain the spectra.

2.5. Composite fabrication

Water hyacinth reinforced PP composites were prepared by using dried UWH and OWH, respectively with PP following the procedure described below:

PP polymer was crushed using a grinding machine. The particle size of the ground PP was mesh 20. The moisture-free dried UWH and OWH were taken and mixed thoroughly with finely divided PP granules to prepare composites in different weight fractions. Composite sheets were prepared with the ratios mentioned in Table 1 by compression molding technique.

2.6. Preparation of composite sheets by compression molding technique

A compression molding machine was employed and the mixture of finely divided granules of PP and water hyacinth powder (WHP) was molded. All composites were prepared by controlling the temperature, pressure, heating, and cooling time at the same rate. Heating time and applied pressure were 10 min and 150–200 kN, respectively. Temperature of the both upper and lower plate was 190 °C. After the completion of curing, heat of both upper and lower plates was turned off. Following an additional 5-min interval, the specimen was cooled down by circulating tap water through the external region of the heating plates of a hydraulic press machine. The length, width and thickness of the composite sheets were around 13 mm, 10.5 mm and 2 mm, respectively. Subsequently, composites were taken out of the mold and were cut into specimens with appropriate dimensions for various tests. Schematic diagram of the manufacturing process is given in Fig. 1.

2.7. Water absorption test of composites

In evaluating the water absorption characteristics of the composites, specimens measuring 39 mm × 10 mm × 2 mm were cut from UWH-PP and OWH-PP composites with diverse weight fractions ranging from 1 % to 10 %. The Established protocol outlined in ASTM D570-99 for water absorption test was followed. In accordance with the ASTM D570-99 standard procedure, specimens were submerged in distilled water for approximately 24 h at room temperature at 25 °C to conduct water absorption tests. After testing three duplicate specimens, the average of the tested specimens is shown in Fig. 11.

2.8. Mechanical properties of the composites

The following tests were conducted to investigate the mechanical properties of the prepared composites: (a) tensile strength; (b) elongation at break; and (c) Izod impact test. The appropriate ASTM procedures were used for carrying out these tests.

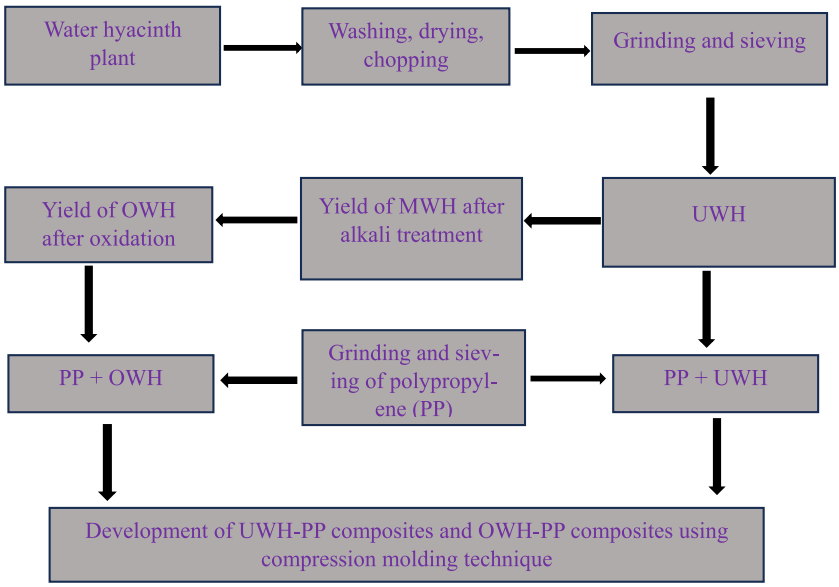

Fig. 1. Schematic diagram of manufacturing process.

2.8.1. Tensile test

At a cross head speed of 10 mm/min, the tensile characteristics of both UWH and OWH reinforced PP composites were evaluated using a universal tensile testing machine (model: 1410-Titans, capacity: 5 kN, England). Except for 100 % PP composite, tensile testing was carried out in accordance with ASTM D 3039/D 3039 M − 00 method and continued until tensile failure occurred. For every composition, six to ten specimens were evaluated, and a maximum of five values were calculated to present the average values.

2.8.2. Izod impact test

Dynamic Izod impact tests of all composites prepared were carried out according to ASTM D256-2, using a Universal Charpy/Izod Analogue Impact Tester (Model: QPI-IC-21 J, Qualitest, North America) machine. Operating parameters of the machine was as follows:

A hammer weighing 4.028 kg, with an impact length of 327 mm, a mass center distance of 0.302 m, an initial angle of 150°, and a free rotatable angle of 148°.

The width, thickness, and length of the composite specimens were 10, 2.5, and 50 mm, respectively and the samples were un-notched. The specimen was held on a vertical simple beam in accordance with the test procedure, and it was broken by a single pendulum swing with the impact line situated precisely halfway between the supports. The average values for each distinct composite were taken from testing five samples.

2.9. Thermal properties analyses

Thermogravimetric analysis (TGA) for both UWH-PP composites and OWH-PP composites was determined by TG-GC-MS (Pyris-Clarus 680- Clsrus SQ8, PerkinElmer, USA) with a heating rate of 15 °C/min under nitrogen atmosphere. TGA curve was obtained for both samples heated from 40 °C to 760 °C.

2.10. Scanning electron microscopy (SEM)

The structure of the fracture surfaces in the tensile samples was investigated using a scanning electron microscope (model: JEOL JSM-6490LA, manufactured by JEOL Ltd., Japan). To facilitate observation, the samples were sectioned into small portions, coated with a layer of gold, and mounted onto holders with the aid of carbon tape. The samples were meticulously focused onto the surfaces and subjected to examination at different magnifications.

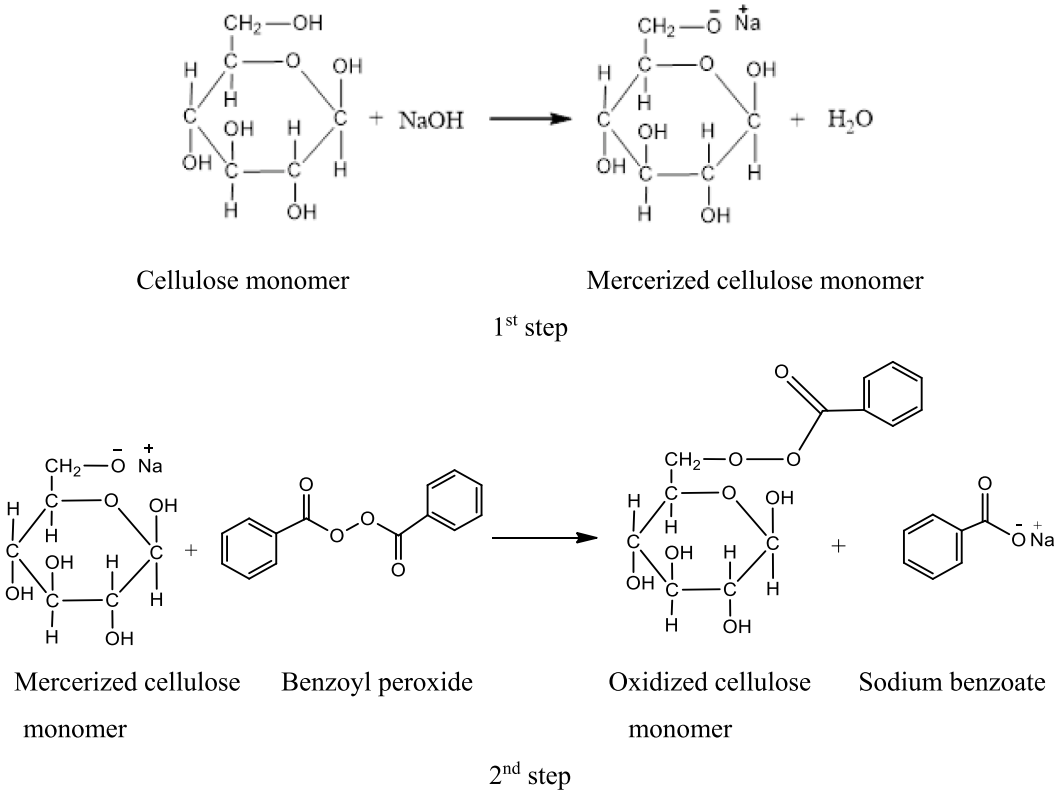

Fig. 2. Reaction scheme of alkali treatment of cellulose in UWH and oxidation of the product with benzoyl peroxide.

3. Computational procedures

DFT level of theory [24] was employed for all calculations along with Becke's 3-parameter hybrid interchange functional (B3LYP) [25] using Gaussian 16 [26] software. Each structure of reactants and products in reactions of step 1 and step 2 (Fig. 2) was fully optimized, which means all bond lengths, bond angles and dihedral angles were allowed to vary during the energy minimization process. Two different basis sets, 6-31+G(d,p) and correlation consistent polarized valence triply-split zeta (cc-pVTZ) were used to optimize the structures. IR frequencies and electronic property such as NBO charge were calculated. The effect of solvent was taken into account using the implicit model- Conductor-like Polarizable Continuum Model (CPCM) [27] approach. For the first step of the reaction scheme (Fig. 2), water was chosen as the solvent, and in the second step, acetone, instead of water, was chosen. Each observed frequency value was multiplied by scaling value of 0.968 as applicable for B3LYP/cc-pVTZ basis set [28]. Reaction energies of both steps were calculated using the following equation-

ΔE = Sum of energies of all products – Sum of energies of all reactants

Similarly, ΔH and ΔG were calculated.

4. Results and discussion

4.1. UWH and OWH characterization

4.1.1. Modification of UWH by benzoyl peroxide

To reduce the hydrophilicity of water hyacinth cellulose, chemical modification was employed, with the reaction being optimized by varying different parameters. In the first step, sodium hydroxide treatment was employed to eliminate lignin from UWH cellulose. This chemical process transforms cellulose into mercerized cellulose. In the second step, the cellulose anhydroglucose unit, where the primary hydroxyl group is at C6, which is more reactive compared to the secondary hydroxyl groups at C2 and C3 [5] undergoes modification, resulting in the production of hydrophobic benzoyloxy cellulose (Fig. 2).

4.1.2. ATR-FTIR spectroscopic characterization of UWH, MWH and OWH compared with the calculated IR spectra

In Fig. 3, the ATR-FTIR spectrum of UWH is compared with the calculated IR spectrum of cellulose monomer. The absorption frequencies, representing different groups, are summarized in Table 2. The broad absorption band at 3334 cm^{-1} indicates the hydrogen-bonded (OH) stretching vibration [29]. The calculated values exceeded the experimental ones because only the isolated cellulose monomer was considered in DFT studies, which could not form intermolecular hydrogen bonding. Notably, the experimental peak at 1247 cm^{-1}, corresponding to the C=O stretch of the acetyl group of lignin, decreased post-modification, highlighting a structural change [19].

Fig. 4 illustrates the ATR-FTIR spectrum of the MWH, along with the calculated spectrum. The absorption frequencies are presented in Table 2. The ATR-FTIR analysis of OWH, compared with the calculated spectrum of oxidized cellulose monomer, is exhibited in Fig. 5, and the absorption frequencies are outlined in Table 2. The ATR-FTIR spectra reveal the absence of an absorption peak at 1866 cm^{-1}, confirming the successful removal of hemicellulose and lignin [23]. In the chemical reaction involving alkali-treated fibers and benzoyl peroxide, a new carbonyl group forms within the cellulose of WHP, evidenced by the absorption peak at 1760 cm^{-1} [18], affirming the chemical modification. The alignment of calculated values with experimental data further validates the modification, particularly the replacement of hydrogen of the hydroxymethyl group with the benzene ring-containing benzoyl group. The hydrophobic nature of the benzene group [23] surpassing that of the hydroxyl group, indicates a reduction in the hydrophilicity of cellulose after chemical modification. Furthermore, the presence of a peak at 1602 cm^{-1} (experimental) and calculated values at 1587 cm^{-1} indicates the introduction of a benzene ring during the chemical modification process [5]. The experimental peak at 1247 cm^{-1} corresponds to the C=O stretch of the acetyl group in lignin, which diminishes following modification [19].

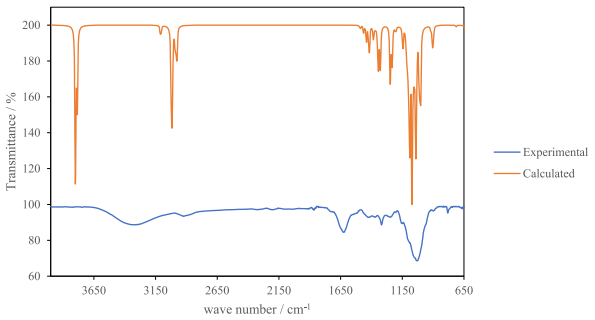

Fig. 3. ATR-FTIR spectrum of UWH compared with the calculated spectrum of Cellulose monomer.

Table 2
Comparison of ATR-FTIR spectral data of UWH, MWH and OWH with calculated vibrational frequencies (cm^{-1}) assignments of monomer of cellulose, mercerized cellulose and oxidized cellulose based on B3LYP/cc-pVTZ basis set.

Molecules	Assignments	Frequency/v cm^{-1} (This work)		Literature value [5,29–32]
		Experimental	Calculated	
Cellulose monomer	ϑ (OH)	3334	3664 (sym)	3400
	ϑ (C–H) in aromatic ring and alkanes	2923	2918 (sym)	2907
Mercerized cellulose monomer	ϑ (OH)	3334	3008 (asym)	3420
	ϑ (C–H) in aromatic ring and alkanes	2950	3644 (sym)	2891
Oxidized cellulose monomer	ϑ (OH)	3342	2665 (asym)	3433.94
	ϑ (C-H)	2914	2721 (asym)	2928.1
	ϑ (C=O)	1760	3679 (sym)	1753
	ϑ (O-O)	892	2951 (sym)	900–800
	ϑ (C-O)	1034	3001 (asym)	1310–1095
	an aromatic ring	1602	1714 (sym)	1600–1450
			918 (sym)	
			1052 (sym)	
			1587 (sym)	

*sym = symmetric stretch; asym = asymmetric stretch.

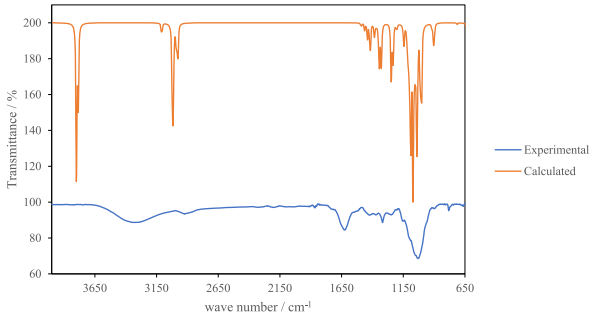

Fig. 4. ATR-FTIR spectrum of MWH compared with calculated spectrum of alkali treated cellulose monomer.

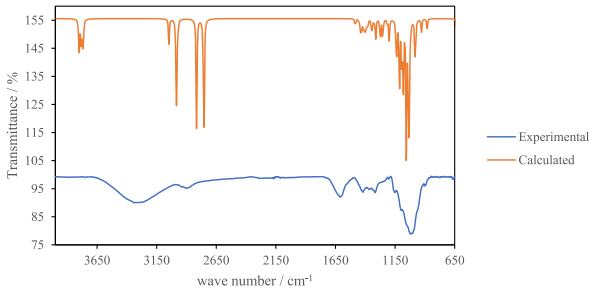

Fig. 5. ATR-FTIR spectrum of OWH compared with calculated spectrum ofoxidized cellulose monomer.

4.1.3. TGA of UWH and OWH

Fig. 6 displays the OWH and UWH TGA curves. There are noticeable differences in thermal behaviors, and OWH shows better thermal stability. Both samples show initial weight loss due to moisture evaporation below 120 °C, but UWH loses more, indicating higher moisture content. The primary decomposition occurs between 250 °C and 450 °C, corresponding to the breakdown of cellulose, hemicellulose, and lignin. UWH decomposes at a lower temperature (~330 °C) compared to OWH (~350 °C), suggesting that treatment improves the thermal resistance of water hyacinth by altering its organic structure. At around 740 °C, minimal additional weight loss is observed for both samples, indicating that the remaining mass consists primarily of thermally stable inorganic materials and carbonaceous residues. OWH retains around 6 % residual mass, whereas UWH retains around 14 % (Fig. 6, suggesting that the treatment reduces the formation of these stable residues. This could be due to structural modifications during the treatment that promote more complete degradation. These findings indicate that treated water hyacinth could be more suitable for applications requiring higher thermal resistance, such as in bio-composites.

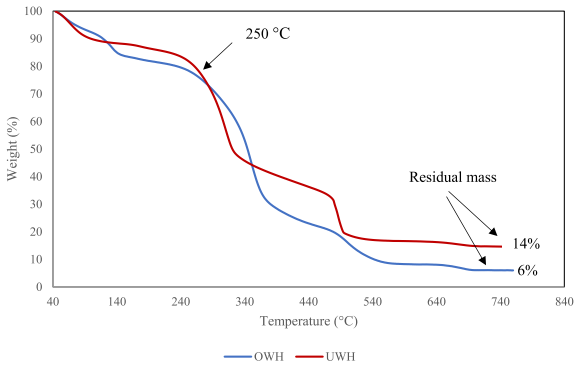

Fig. 6. TGA curves for UWH and OWH.

4.2. *Mechanical properties of UWH and OWH reinforced PP composites*

Tensile strength, elongation at break, impact strength of the UWH and OWH reinforced PP composites have been assessed using standard ASTM methods. The findings are presented below.

4.2.1. *Tensile strength and elongation at break*

The tensile strength and elongation at break of compression molded pure PP sheet specimen are measured as 28.57 MPa and 17.47 %, respectively. The tensile strength and elongation at break for all the composites are shown in Figs. 7 and 8. The tensile strength value for UWH-PP composites increases initially and gives the best value for 1 % reinforcement. For OWH-PP composites, the tensile strength value is higher for 1 % reinforcement as well. From Fig. 7, it is observed that the tensile strengths of the OWH-PP composites are greater than those of UWH-PP composites. However, the tensile strength of OWH-PP composites drops with increasing WHP loading. This might stem from inadequate stress transfer from the PP matrix to the biopolymer WHP.

The enhancement in tensile strength at 1 % fiber loading can be attributed to strong fiber-matrix adhesion, facilitating consistent stress transfer from the matrix to the reinforcing fiber [33]. Conversely, the decline in tensile strength at higher fiber loadings results from weak fiber-matrix adhesion, leading to debonding during tensile testing. This debonding may create voids, fostering the easy spread of defects in void-containing regions. Additionally, uneven fiber dispersion in the composites, coupled with fiber aggregation within the matrix, further influences tensile strength The non-uniform stress transfer, stemming from irregular fiber orientation in the matrix, contributes to the observed variations.

As the proportion of fibers increases, the elongation at break decreases. This reduction in elongation at break is attributed to the limited elasticity and flexibility exhibited by the fibers within the composites. Additionally, heightened rigidity and toughness accompany this change, whereas ductility experiences a decline [34]. In a study by Haque et al., polypropylene composites reinforced with short WHP fibers, spanning concentrations from 5 % to 30 %, their observations align with the general trend, showcasing a decline in elongation at break with escalating fiber content. The findings indicated a diminishing trend in elongation at break as the fiber content increased [35].

Fig. 8 shows that the elongation decreases with increasing WHP loading (wt. %). But comparatively, OWH-PP composites have a lower elongation at break values than the corresponding elongation at break values of UWH-PP composites. Low elongation at break means the material doesn't stretch much before breaking. It undergoes minimal deformation or elongation before reaching the point of rupture. When biopolymers are added to synthetic polymers, the elongation at break tends to decrease. This is primarily due to the reinforcing effect of the biopolymers, which make the composite material stiffer and less flexible [36].

The presence of WHP as filler restricts the movement of polymer chains, limiting their ability to undergo plastic deformation and decreasing elongation at break. Elongation exhibits an inverse relationship with a material's tensile strength, hardness and modulus.

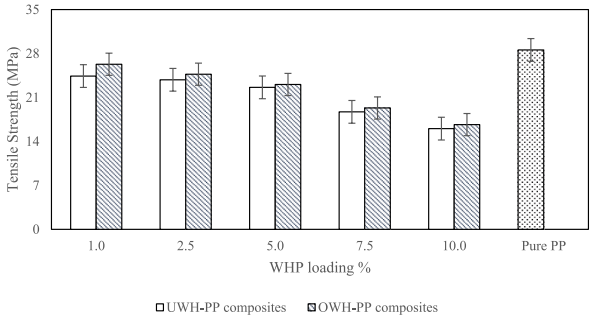

Fig. 7. Tensile strength vs WHP loading (wt. %) bars for UWH-PP and OWH-PP composites.

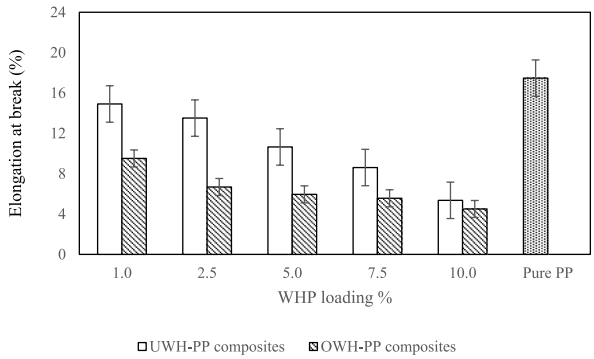

Fig. 8. Elongation at break vs WHP loading (wt. %) bars for UWH-PP and OWH-PP composites.

Brostow and Lobland [37] have indicated that elongation and impact strength are inversely proportionate to brittleness. They emphasize the significance of assessing the brittleness of polymers and polymer-based materials for establishing their suitability in various applications. The toughness or ductility of composites rises with an increase in elongation at break. Therefore, an elevated elongation in composites indicates a reduction in brittleness.

4.2.2. Izod impact strength

Compared to some UWH and OWH reinforced PP composites, a 100 % polypropylene (PP) composite has a lower impact strength of 15.13 J/m. The Izod impact strength of the UWH-PP and OWH-PP composites is shown in Fig. 9. As seen in the figure, some of the values are higher than those of PP polymer that isn't filled. Impact strength increases as the fiber loading drops to 1 %. Additionally, benzoyl peroxide-treated composites exhibit better results compared to UWH-PP composites, showcasing the effectiveness of the treatment.

The improvement in impact strength is largely due to the addition of WHP as a filler in the PP matrix. Fillers are essential for enhancing the performance of composite materials, and in this case, WHP significantly strengthens the structure and improves impact strength.

WHP's high cellulose content contributes to the overall strength of the composite, while its compatibility with PP facilitates a strong bond between the filler and the matrix. This connection enhances load transfer and improves impact resistance. Additionally, WHP plays a critical role in absorbing and distributing impact strength, thereby reducing the risk of cracks and material failure.

According to Brostow and Lobland, a material's impact strength is inversely correlated with its brittleness, and the lower the brittleness, the higher its dimensional stability [38]. The relationship between hardness and impact strength in composite materials is inversely proportional [39]. Treating WHP with benzoyl peroxide enhances the fracture resistance of OWH-PP composites, resulting in a reduction in their brittleness.

It is important to note that as WHP loading increases, the Izod impact strength decrease. Higher WHP content can lead to increased brittleness in the material, reducing its capacity to absorb impact energy.

4.2.3. Effect of surface modification of fibers on the mechanical properties of treated WHP reinforced PP composites

The mechanical properties of benzoyl peroxide-OWH-PP composites show significant improvement compared to UWH-PP composites. This enhancement can be explained by the hydrophilic nature of WHP and the hydrophobic nature of the PP matrix. The hydrophilic WHP fiber exhibits relatively weak interfacial adhesion to the hydrophobic PP matrix. The treatment of WHP fibers leads to a decrease in their hydrophilic characteristics when compared to UWH fibers. The treated WHP exhibits increased interfacial

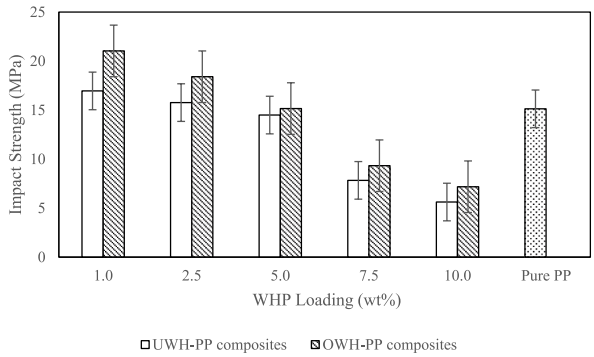

Fig. 9. Impact strength (MPa) versus WHP loading (wt %) bars for UWH-PP and OWH-PP composite.

adhesion to the PP matrix due to its hydrophobic property. The enhanced bonding at the interface between chemically treated WHP and the PP matrix in OWH-PP composites contributes to the increase in their mechanical properties compared to UWH-PP composites.

4.3. Thermogravimetric analysis (TGA)

Thermogravimetric analyses (TGA) were conducted on 2.5 % UWH-PP and OWH-PP composites and pure PP specimens illustrated in Fig. 10. The results reveal a three-stage thermal degradation process. Initial weight loss occurred at temperatures below 100 °C. The first degradation stage for both UWH-PP and OWH-PP unfolds between 40 °C and 255 °C, with a modest 3 % weight loss in this temperature span, whereas for pure PP, it ranges between 40 °C and 304 °C. Subsequently, for UWH-PP and OWH-PP, the second degradation stage takes place within the temperature range of 260 °C–385 °C, exhibiting a substantial 92 % weight loss. The final degradation stage manifests in the temperature range of 397 °C–758 °C, leaving very little ash content. Fig. 10 distinctly illustrates that the thermal stability of OWH-PP closely aligns with that of UWH-PP, indicating comparable results and stability. From the results, there is no significant difference in the degradation process between UWH-PP and OWH-PP composites. However, the temperature range is slightly lower than that of virgin PP because of the incorporation of fibers in the matrix.

4.4. Water absorption

To investigate the impact of water absorption, UWH-PP and OWH-PP composites at various weight fractions (1–10 wt%) were prepared. Fig. 11 illustrates the measured impact of water absorption on the OWH and UWH loading on the WHP–PP composites. It shows that as the fiber loading of the composite increases, so does their water absorption. Additionally, the figure shows that OWH-PP composites absorb less water than UWH-PP composites. It might be because UWH contains cellulose and lignin, both of which have hydroxyl groups that can interact with water molecules to form hydrogen bonds. The figure also shows that, in comparison to UWH-PP composites, OWH-PP composites had a significant decrease in hydrophilicity. Given that benzoyl groups are more hydrophobic than hydroxyl groups, the addition of benzoyloxy groups may be the cause of this decrease in hydrophilicity of the cellulose derivative. The mechanical properties and dimension stability of OWH-PP composites are enhanced by decreased absorption of water. An appropriate chemical treatment can reduce water absorption and improve the mechanical properties and stability of natural fiber reinforced composites, making them more durable [40].

4.5. Morphological analysis

To examine the surface characteristics of the prepared composites, scanning electron micrographs (SEM) were taken using 2.5 wt-% UWH-PP and OWH-PP composites. SEM images of scratched portions from the fracture surfaces of tensile test specimens are displayed in Figs. 12–14. The SEM analysis of the UWH-PP composite reveals a deficiency in interfacial interaction, leading to inadequate adhesion between the UWH and the PP matrix. This lack of interaction is attributed to the intermolecular hydrogen bond formation between WHP and the hydrophobic PP matrix. Consequently, the hydrophilic WHP tends to agglomerate into bundles, resulting in uneven distribution throughout the matrix.

Examining the SEM images of the OWH-PP composite reveals enhanced interfacial adhesion between the OWH fiber and the PP matrix compared to the UWH-PP composite. In the UWH-PP composite, the UWH shows weak dispersion due to intermolecular hydrogen bonding and agglomeration. On the contrary, the OWH contains benzoyloxy groups that cannot form intermolecular hydrogen bonds, leading to uniform dispersion in the OWH-PP composites. This improved interfacial bonding in the OWH-PP

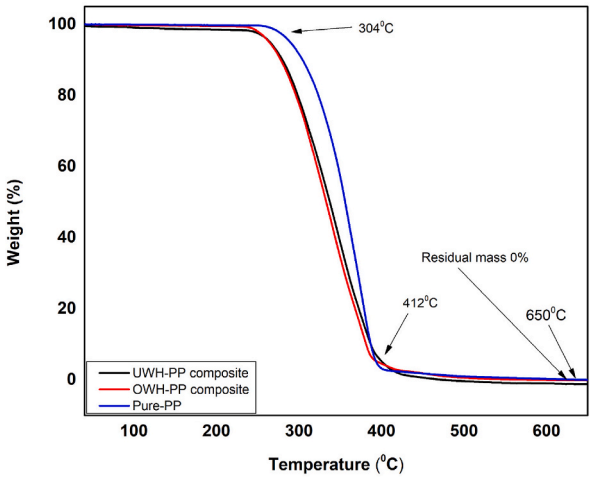

Fig. 10. TGA curves for 2.5 % UWH-PP and OWH-PP composites and Pure PP.

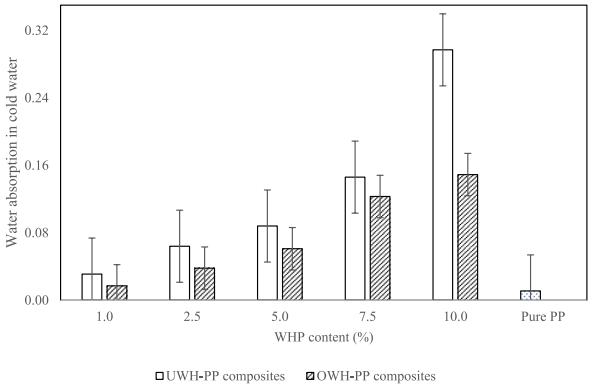

Fig. 11. Cold water absorption (%) versus WHP loading (%) bars for PP, UWH-PP and OWH-PP composites.

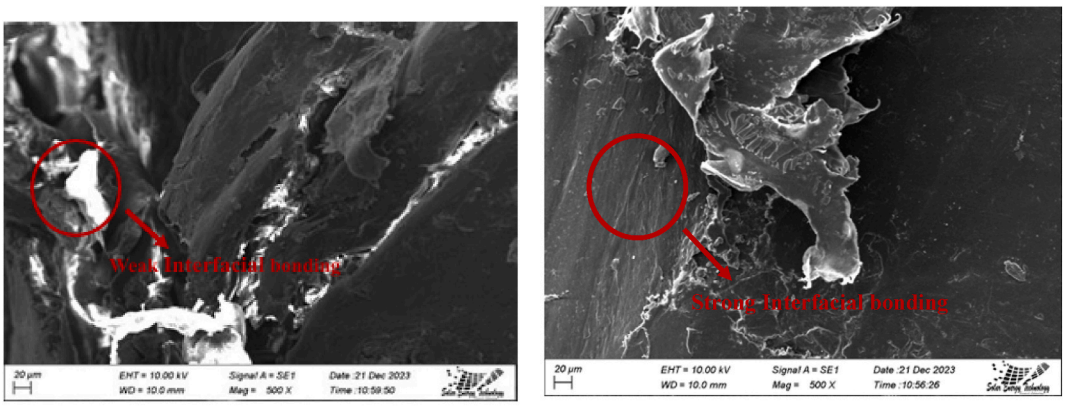

Fig. 12. (a) SEM micrograph (20 μm) of 2.5 wt-% UWH-PP composite and (b) SEM micrograph (20 μm) of 2.5 wt-% OWH-PP composite.

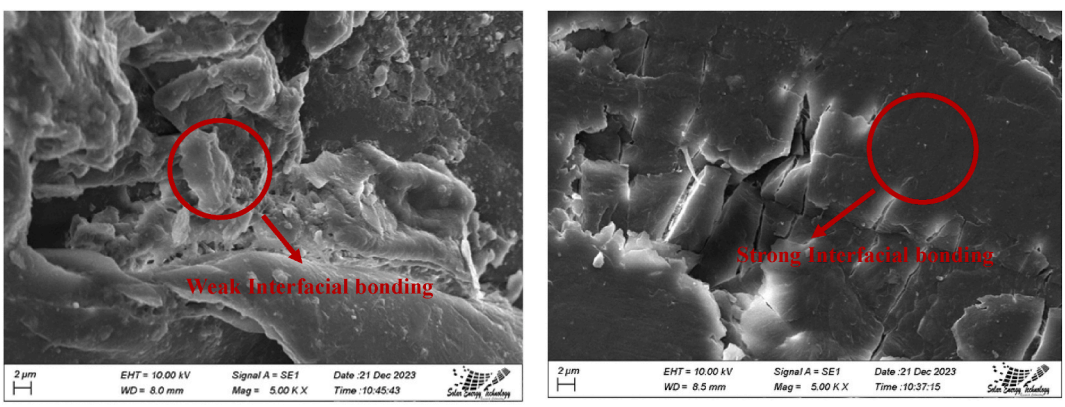

Fig. 13. (a) SEM micrograph (2 μm) of 2.5 wt-% UWH-PP composite and (b) SEM micrograph (2 μm) of 2.5 wt-% OWH-PP composite.

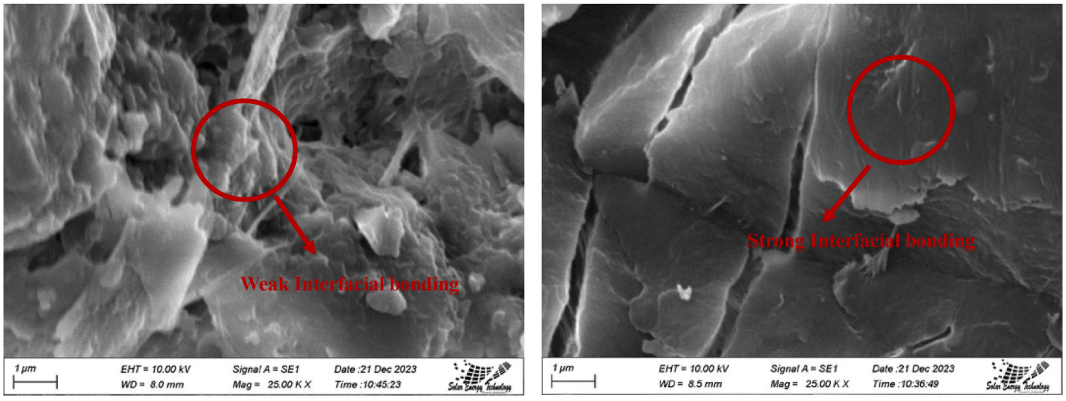

Fig. 14. (a) SEM micrograph (1 μm) of 2.5 wt-% UWH-PP composite and (b) SEM micrograph (1 μm) of 2.5 wt-% OWH-PP composite.

composite is more evident in the figures than in the UWH-PP composite.

4.6. Energy and thermodynamic properties from computational methods

The reaction energy (ΔE), enthalpy (ΔH) and free energy change (ΔG) of each step of the reaction are shown in Tables 3 and 4, respectively. The reaction of cellulose monomer with NaOH in water shows negative values for ΔE, ΔH and ΔG (Table 3). These negative values suggest feasibility for the first step of reaction scheme. The second step of the reaction scheme involving mercerized cellulose and benzoyl peroxide as reactants, is much more feasible as the free energy and enthalpy change along with reaction energy is much more negative (Table 4).

The free energy diagram of the reaction is illustrated in Fig. 15. The diagram shows relative difference between ΔG_1.in the first step, ΔG_2 from the second step. These observations collectively show that the reaction is thermodynamically feasible.

4.7. Electronic properties

NBO charges of the selected atoms of some optimized structures are presented in Fig. 16. From Fig. 16, it can be seen that there is a change in the negative charge on the oxygen atom of the O-O group in benzoyl peroxide, from −0.239 to −0.264, indicates a charge transfer when it forms a bond with the oxygen of the -CH_2OH group during the reaction with the cellulose monomer. This charge transfer results in a higher charge density between the oxygen atoms in the O-O group of the oxidized cellulose monomer compared to benzoyl peroxide. The higher charge density is associated with a stronger O-O bond in the oxidized cellulose monomer, as it is evident by the higher experimental IR frequency of 892 cm^{-1} found in this study (Table 2), compared to 833 cm^{-1} in isolated benzoyl peroxide [41]. Furthermore, the change in negative charge on the oxygen atom of the -CH_2OH group, from −0.041 to −0.067 has been found. These altogether suggest that the reaction leads to the oxidation of the cellulose monomer, forming an oxidized cellulose monomer.

5. Conclusion

To improve adhesion in WHP-PP composites, benzoyl peroxide treatment was applied to water hyacinth (Eichhornia crassipes). The process involved alkali pretreatment of UWH, followed by additional benzoyl peroxide treatment. Compared with calculated (DFT) vibrational spectra, ATR-FTIR spectra confirmed cellulose modification in UWH to OWH, reducing the hydrophilic tendency of water hyacinth fibers and decreasing water absorption in treated composites. Benzoyl peroxide treatment significantly enhanced mechanical properties in OWH-PP composites, with improved tensile strength, elongation at break, and impact strength compared to UWH-PP composites. This treatment demonstrated increased resistance against brittle deformation and fracture in the composites. Thermogravimetric analysis shows promising thermal degradation process of the composites. Additionally, water absorption properties improved, enhancing dimensional stability in OWH-PP composites. Morphological studies of these composites show better interfacial bonding between fiber and matrix for OWH-PP composites than UWH-PP composites. DFT calculations revealed favourable thermodynamic properties, with negative energy, enthalpy, and free energy. In conclusion, modifying alkali pre-treated water hyacinth

Table 3
Reaction energy, enthalpy and free energy change of step 1 in water medium.

Basis set	ΔE/kJ mol^{-1}	ΔH/kJ mol^{-1}	ΔG/kJ mol^{-1}
6-31G+(d,p)	−0.85	−0.43	−0.18
cc-pVTZ	−2.38	−2.08	−1.99

Table 4
Reaction energy, enthalpy and free energy change of step 2 in acetone solvent.

Basis set	ΔE/kJ mol^{-1}	ΔH/kJ mol^{-1}	ΔG/kJ mol^{-1}
6-31G+(d,p)	−32.79	−31.89	−32.79
cc-pVTZ	−31.55	−30.69	−32.42

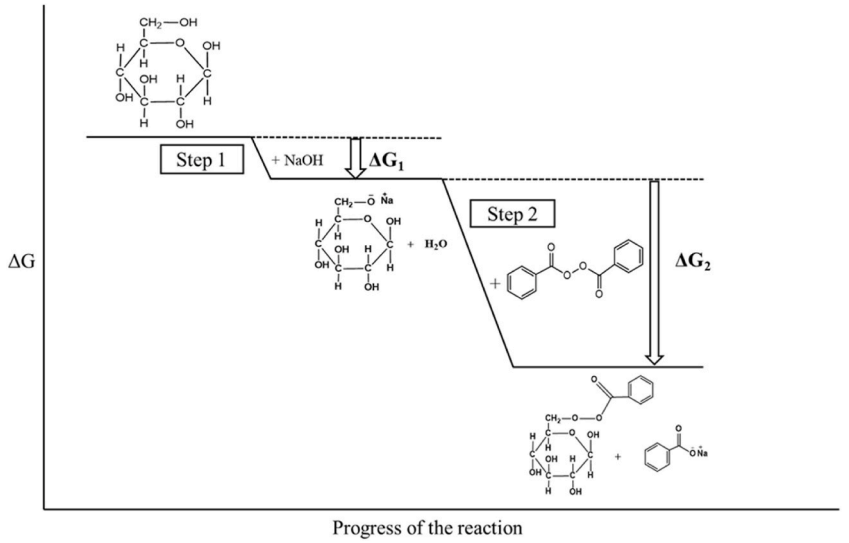

Fig. 15. Free energy diagram of the reaction.

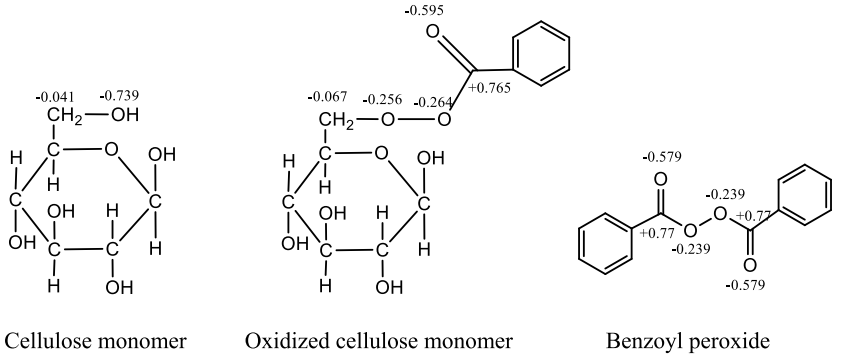

Fig. 16. NBO charges on selected atoms of Cellulose monomer, Oxidized cellulose monomer and Benzoyl peroxide.

with benzoyl peroxide enhanced physico-mechanical properties and exhibited promising thermodynamic characteristics. These results pave the way for further exploration in developing advanced materials with superior performance, contributing to the sustainable and eco-friendly evolution of materials for diverse applications.

CRediT authorship contribution statement

Kaniz Fatema: Writing – original draft, Validation, Methodology, Investigation, Formal analysis, Data curation. **Taslima Akter:** Methodology, Investigation, Formal analysis, Data curation. **Zahidul Islam:** Validation, Methodology, Formal analysis, Data curation. **Mohammad Shahriar Bashar:** Methodology, Formal analysis, Data curation. **Shahin Sultana:** Writing – review & editing, Supervision, Methodology, Investigation, Formal analysis, Data curation, Conceptualization. **M. Saiful Islam:** Writing – review & editing, Supervision, Investigation, Conceptualization.

Data availability

The corresponding author will provide the datasets generated and analyzed in this study upon reasonable request.

Declaration of competing interest

The authors declare the following financial interests/personal relationships which may be considered as potential competing interests:The authors have disclosed no conflicts of interest. If there are other authors, they declare that they have no known competing financial interests or personal relationships that could have appeared to influence the work reported in this paper.

Acknowledgments

The authors would like to thank the Bangladesh Council of Scientific and Industrial Research (BCSIR) for providing the laboratory facilities.

References

[1] S. Mahmud, K.M.F. Hasan, M.A. Jahid, K. Mohiuddin, R. Zhang, J. Zhu, Comprehensive review on plant fiber-reinforced polymeric biocomposites, J. Mater. Sci. 56 (2021) 7231–7264, https://doi.org/10.1007/s10853-021-05774-9.
[2] A. Shalwan, B.F. Yousif, In state of art: mechanical and tribological behaviour of polymeric composites based on natural fibres, Mater. Des. 48 (2013) 14–24, https://doi.org/10.1016/j.matdes.2012.07.014.
[3] J. Holbery, D. Houston, Natural-fiber-reinforced polymer composites in automotive applications, Jom 58 (2006) 80–86.
[4] R. Kumar, M.I. Ul Haq, A. Raina, A. Anand, Industrial applications of natural fibre-reinforced polymer composites–challenges and opportunities, Int. J. Sustain. Eng. 12 (2019) 212–220, https://doi.org/10.1080/19397038.2018.1538267.
[5] T. Akter, H.P. Nur, S. Sultana, M.R. Islam, M.J. Abedin, Z. Islam, Evaluation of mechanical properties of both benzoyl peroxide treated and untreated teak sawdust reinforced high density polyethylene composites, Cellulose 25 (2018) 1171–1184, https://doi.org/10.1007/s10570-017-1620-3.
[6] H.A. Maddah, Polypropylene as a promising plastic: a review, Am. J. Polym. Sci. 6 (2016) 1–11, https://doi.org/10.5923/j.ajps.20160601.01.
[7] S. Spoljaric, A. Genovese, R.A. Shanks, Polypropylene-microcrystalline cellulose composites with enhanced compatibility and properties, Compos Part A Appl Sci Manuf 40 (2009) 791–799, https://doi.org/10.1016/j.compositesa.2009.03.011.
[8] R. Sindhu, P. Binod, A. Pandey, A. Madhavan, J.A. Alphonsa, N. Vivek, E. Gnansounou, E. Castro, V. Faraco, Water hyacinth a potential source for value addition: an overview, Bioresour. Technol. 230 (2017) 152–162, https://doi.org/10.1016/j.biortech.2017.01.035.
[9] P.L. Bolorunduro, Water hyacinth infestation: nuisance or nugget, in: Proceedings of the International Conference on Water Hyacinth, 2002, pp. 111–121. New Bussa, Nigeria.
[10] T. Jirawattanasomkul, H. Minakawa, S. Likitlersuang, T. Ueda, J.G. Dai, N. Wuttiwannasak, N. Kongwang, Use of water hyacinth waste to produce fibre-reinforced polymer composites for concrete confinement: mechanical performance and environmental assessment, J. Clean. Prod. 292 (2021), https://doi.org/10.1016/j.jclepro.2021.126041.
[11] M. Mohammed, A.J.M. Jawad, A.M. Mohammed, J.K. Oleiwi, T. Adam, A.F. Osman, O.S. Dahham, B.O. Betar, S.C.B. Gopinath, M. Jaafar, Challenges and advancement in water absorption of natural fiber-reinforced polymer composites, Polym. Test. 124 (2023), https://doi.org/10.1016/j.polymertesting.2023.108083.
[12] T.H. Mokhothu, M.J. John, Bio-based coatings for reducing water sorption in natural fibre reinforced composites, Sci. Rep. 7 (2017), https://doi.org/10.1038/s41598-017-13859-2.
[13] S. Sanjeevi, V. Shanmugam, S. Kumar, V. Ganesan, G. Sas, D.J. Johnson, M. Shanmugam, A. Ayyanar, K. Naresh, R.E. Neisiany, O. Das, Effects of water absorption on the mechanical properties of hybrid natural fibre/phenol formaldehyde composites, Sci. Rep. 11 (2021), https://doi.org/10.1038/s41598-021-92457-9.
[14] T.H. Mokhothu, M.J. John, Bio-based coatings for reducing water sorption in natural fibre reinforced composites, Sci. Rep. 7 (2017), https://doi.org/10.1038/s41598-017-13859-2.
[15] A.Y. Al-Maharma, N. Al-Huniti, Critical review of the parameters affecting the effectiveness of moisture absorption treatments used for natural composites, Journal of Composites Science 3 (2019), https://doi.org/10.3390/jcs3010027.
[16] T.D. Tavares, J.C. Antunes, F. Ferreira, H.P. Felgueiras, Biofunctionalization of natural fiber-reinforced biocomposites for biomedical applications, Biomolecules 10 (2020), https://doi.org/10.3390/biom10010148.
[17] N. Karthi, K. Kumaresan, S. Sathish, S. Gokulkumar, L. Prabhu, N. Vigneshkumar, An overview: natural fiber reinforced hybrid composites, chemical treatments and application areas, in: Mater Today Proc, Elsevier Ltd, 2019, pp. 2828–2834, https://doi.org/10.1016/j.matpr.2020.01.011.
[18] M. Masłowski, J. Miedzianowska, K. Strzelec, Influence of peroxide modifications on the properties of cereal straw and natural rubber composites, Cellulose 25 (2018) 4711–4728, https://doi.org/10.1007/s10570-018-1880-6.
[19] K.V. Kumar, A.A.M. Moshi, J.S. Rajadurai, Mechanical property analysis on bamboo-glass fiber reinforced hybrid composite structures under different lamina orders, in: Mater Today Proc, Elsevier Ltd, 2021, pp. 1620–1625, https://doi.org/10.1016/j.matpr.2020.08.423.
[20] M. Haque, N. Islam, M. Huque, M. Hasan, S. Islam, S. Islam, Coir fiber reinforced polypropylene composites: physical and mechanical properties, Adv. Compos. Mater. 19 (2010) 91–106.
[21] N. Sumrith, L. Techawinyutham, M.R. Sanjay, R. Dangtungee, S. Siengchin, Characterization of alkaline and silane treated fibers of 'water hyacinth plants' and reinforcement of 'water hyacinth fibers' with bioepoxy to develop fully biobased sustainable ecofriendly composites, J. Polym. Environ. 28 (2020) 2749–2760, https://doi.org/10.1007/s10924-020-01810-y.
[22] N. Flores Ramirez, Y. Sanchez Hernandez, J. Cruz de Leon, S.R. Vasquez Garcia, L. Domratcheva Lvova, L. Garcia Gonzalez, Composites from water hyacinth (Eichhornea crassipe) and polyester resin, Fibers Polym. 16 (2015) 196–200.
[23] V.K. Kaushik, A. Kumar, S. Kalia, Effect of mercerization and benzoyl peroxide treatment on morphology, thermal stability and crystallinity of sisal fibers, Int. J. Textil. Sci. 1 (2013) 101–105, https://doi.org/10.5923/j.textile.20120106.07.
[24] I.B. Obot, D.D. Macdonald, Z.M. Gasem, Density functional theory (DFT) as a powerful tool for designing new organic corrosion inhibitors: Part 1: an overview, Corros Sci 99 (2015) 1–30, https://doi.org/10.1016/j.corsci.2015.01.037.
[25] J. Tirado-Rives, W.L. Jorgensen, Performance of B3LYP density functional methods for a large set of organic molecules, J Chem Theory Comput 4 (2008) 297–306, https://doi.org/10.1021/ct700248k.
[26] S. McArdle, S. Endo, A. Aspuru-Guzik, S.C. Benjamin, X. Yuan, Quantum computational chemistry, Rev. Mod. Phys. 92 (2020), https://doi.org/10.1103/RevModPhys.92.015003.
[27] Y. Takano, K.N. Houk, Benchmarking the conductor-like polarizable Continuum model (CPCM) for aqueous solvation free energies of neutral and ionic organic molecules, J Chem Theory Comput 1 (2005) 70–77, https://doi.org/10.1021/ct049977a.

[28] A.F. Rodrigues-Oliveira, F.W.M. Ribeiro, G. Cervi, T.C. Correra, Evaluation of common theoretical methods for predicting infrared multiphotonic dissociation vibrational spectra of intramolecular hydrogen-bonded ions, ACS Omega 3 (2018) 9075–9085, https://doi.org/10.1021/acsomega.8b00815.
[29] D.L. Pavia, G.M. Lampman, G.S. Kriz, J.R. Vyvyan, in: INTRODUCTION TO SPECTROSCOPY, n.d, fourth ed., Brooks/Cole, Belmont, CA, 2009, pp. 70–86.
[30] S.S. Kamath, B. Bennehalli, Surface modification of areca fibre by benzoyl peroxide and mechanical behaviour of areca-epoxy composites, Material Science Research India 18 (2021) 48–55, https://doi.org/10.13005/msri/180106.
[31] M. Tsuboi, Infrared spectrum and crystal structure of cellulose, J. Polym. Sci. 25 (1957) 159–171.
[32] R.H. Marchessault, C.Y. Liang, Infrared spectra of crystalline polysaccharides. III. Mercerized cellulose, J. Polym. Sci. 43 (1960) 71–84.
[33] A. Ramachandran, S. Mavinkere Rangappa, V. Kushvaha, A. Khan, S. Seingchin, H.N. Dhakal, Modification of fibers and matrices in natural fiber reinforced polymer composites: a comprehensive review, Macromol. Rapid Commun. 43 (2022) 2100862.
[34] L.T. Drzal, M. Madhukar, Fibre-matrix adhesion and its relationship to composite mechanical properties, J. Mater. Sci. 28 (1993) 569–610.
[35] H.U. Zaman, R.A. Khan, M. Haque, M.A. Khan, A. Khan, T. Huq, N. Noor, M. Rahman, K. Mustafizur Rahman, D. Huq, Mohamad Asri Ahmad, Preparation and mechanical characterization of jute reinforced polypropylene/natural rubber composite, J. Reinforc. Plast. Compos. 29 (2010) 3064–3065, https://doi.org/10.1177/0731684410364680.
[36] M.S.B. Reddy, D. Ponnamma, R. Choudhary, K.K. Sadasivuni, A comparative review of natural and synthetic biopolymer composite scaffolds, Polymers 13 (2021), https://doi.org/10.3390/polym13071105.
[37] W. Brostow, H.E. Hagg Lobland, Brittleness of materials: implications for composites and a relation to impact strength, J. Mater. Sci. 45 (2010) 242–250, https://doi.org/10.1007/s10853-009-3926-5.
[38] W. Brostow, H.E. Hagg Lobland, Survey of relations of chemical constituents in polymer-based materials with brittleness and its associated properties, Chemistry and Chemical Technology 10 (2016) 595–600, https://doi.org/10.23939/chcht10.04si.595.
[39] A. Aruniit, J. Kers, A. Krumme, P. Peetsalu, Particle size and proportion influence to impact properties of particulate polymer composite, in: 9th International DAAAM Baltic Conference Industrial Engineering, 2014, pp. 24–26.
[40] A.A. Bachchan, P.P. Das, V. Chaudhary, Effect of moisture absorption on the properties of natural fiber reinforced polymer composites: a review, in: Mater Today Proc, Elsevier Ltd, 2020, pp. 3403–3408, https://doi.org/10.1016/j.matpr.2021.02.812.
[41] J.S. Al-Otaibi, Molecular structure, spectroscopic (FT-IR, FT-Raman) and homo–lumo analyses of some acne vulgaris drugs, Rasayan Journal of Chemistry 11 (2018) 88–102, https://doi.org/10.7324/RJC.2018.1111980.